Anomalous Acoustic Plasmon Mode from Topologically Protected States

Xun Jia,[1,2] Shuyuan Zhang,[1,2] Raman Sankar,[3,4] Fang-Cheng Chou,[4] Weihua Wang,[1] K. Kempa,[5] E. W. Plummer,[6] Jiandi Zhang,[6] Xuetao Zhu,[1,2,*] and Jiandong Guo[1,2,7,†]

[1]*Beijing National Laboratory for Condensed Matter Physics and Institute of Physics, Chinese Academy of Sciences, Beijing 100190, China*

[2]*School of Physical Sciences, University of Chinese Academy of Sciences, Beijing 100049, China*

[3]*Institute of Physics, Academia Sinica, Taipei 11529, Taiwan*

[4]*Centre for Condensed Matter Sciences, National Taiwan University, Taipei 10617, Taiwan*

[5]*Department of Physics, Boston College, Chestnut Hill, Massachusetts 02467, USA*

[6]*Department of Physics and Astronomy, Louisiana State University, Baton Rouge, Louisiana 70808, USA*

[7]*Collaborative Innovation Center of Quantum Matter, Beijing 100871, China*

(Received 6 June 2017; revised manuscript received 8 August 2017; published 28 September 2017)

Plasmons, the collective excitations of electrons in the bulk or at the surface, play an important role in the properties of materials, and have generated the field of "plasmonics." We report the observation of a highly unusual acoustic plasmon mode on the surface of a three-dimensional topological insulator (TI) Bi_2Se_3, using momentum resolved inelastic electron scattering. In sharp contrast to ordinary plasmon modes, this mode exhibits almost linear dispersion into the second Brillouin zone and remains prominent with remarkably weak damping not seen in any other systems. This behavior must be associated with the inherent robustness of the electrons in the TI surface state, so that not only the surface Dirac states but also their collective excitations are topologically protected. On the other hand, this mode has much smaller energy dispersion than expected from a continuous media excitation picture, which can be attributed to the strong coupling with surface phonons.

DOI: 10.1103/PhysRevLett.119.136805

A plasmon is a quantum of collective oscillations of charge density due to the restoring force arising from the long-range Coulomb interactions in a solid, predicted in 1951 by Pines and Bohm [1]. The concept was extended to surfaces and interfaces in the form of surface plasmons by Ritchie in 1957 [2]. The properties of plasmons have been studied for over 60 years and have spawned the field of plasmonics and many technological applications. A seminal feature of any plasmon mode, which is important for applications, is its lifetime. In ordinary materials plasmons usually appear in only small momentum ranges, because they can interact with the single-particle excitations (so-called Landau damping) [3,4] when the plasmon energy and momentum overlap the electron-hole pair continuum (EHPC). Even for a plasmon with energy and momentum outside the EHPC there are other damping channels [5,6], such as impurity scattering that increases with increasing momentum. This is true for all plasmon modes, originating from either electron gases in a parabolic band or Dirac massless electrons in a linear band. One example is the two-dimensional (2D) plasmon mode from Dirac electrons in graphene [7], which shows strong damping and diminishes before merging into the EHPC at a small momentum compared to the Brillouin zone (BZ) boundary. In contrast, we demonstrate that an anomalous acoustic surface plasmon mode from the Dirac electrons on the surface of a prototypical three-dimensional (3D) topological insulator Bi_2Se_3 exists even in the second BZ with unusually weak damping and narrow spectral linewidth, which likely relates to the spin-momentum locking feature of the TI surface states. This mode has significantly lower energy than that within the continuous medium excitation picture, indicating the existence of a bosonic coupling. Probably, the mode is dressed by a surface phonon due to strong electron-lattice interactions.

In the case of the Dirac states [8–10] at the surface of topological insulators (TIs) the unconventional spin textures protect the Dirac electrons against scattering from any nonmagnetic impurity [11–13], resulting in a long lifetime for electrons in Dirac states. A relevant question is whether the bosonic collective modes from the electrons in these protected states, such as plasmons, have longer lifetimes than those from topologically trivial metallic states [14]. It has been proposed that the spin texture of Dirac electrons on a 3D TI surface may generate an undamped spin density wave, which can coherently couple to the charge density oscillations (i.e., plasmon) and gives rise to the so-called spin-plasmon mode [15]. At the present time the existing experimental results for plasmon modes on TI surfaces are rather controversial [16–19] and none of them provides direct evidence for the long lifetime characteristic of bosonic collective modes.

The single crystalline samples used here were Bi_2Se_3 [20]. The properties of the samples have been characterized by both transport and spectroscopic measurements [21]. The *in situ* cleaved (0001) surface is terminated with a

 © 2017 American Physical Society

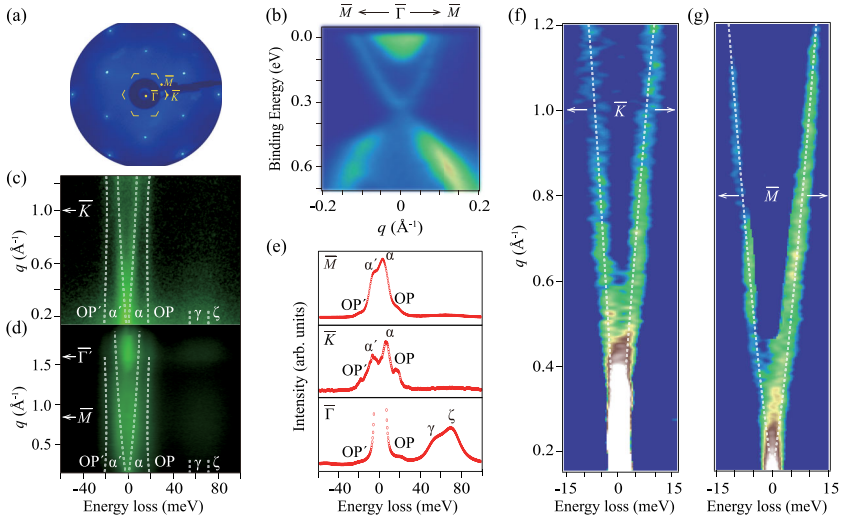

FIG. 1. Experimental results of Bi_2Se_3 (0001). (a) LEED pattern of Bi_2Se_3 (0001) surface with incident energy of 80 eV at room temperature. The red dashed line is the first BZ of Bi_2Se_3 (0001), and the red dots show the high-symmetry points. (b) The band structure along the $\bar{M}-\bar{\Gamma}-\bar{M}$ direction measured by ARPES at 35 K, which shows the coexistence of the bulk conducting band and the V-shaped surface Dirac state. (c) 2D energy-momentum mapping of HREELS along the $\bar{\Gamma}-\bar{K}$ direction with incident energy of 60 eV and (d) along the $\bar{\Gamma}-\bar{M}$ direction with incident energy of 110 eV. Four collective modes with energy loss features are labeled by α, OP, γ, and ζ, respectively. The gray dashed lines are provided to guide to eye. The corresponding negative energy loss features are antistocks peaks of α, OP modes, respectively, which are labeled by α', OP′. (e) EDCs at $\bar{\Gamma}$, $\bar{K}$, and $\bar{M}$ with the corresponding energy loss peaks labeled. (f) and (g) The second derivative image of (c) and (d), respectively, with elastic background removed.

Se layer and its $p(1\times1)$ structure is characterized by low energy electron diffraction (LEED), shown in Fig. 1(a). The band structure is confirmed by the mapping of both the linearly dispersed topological Dirac surface states and parabolic bulk conducting band partly below the Fermi energy [Fig. 1(b)], using *in situ* angle-resolved photoemission spectroscopy (ARPES). The plasmons and other collective excitations, such as phonons, were measured with a newly developed high resolution electron energy loss spectroscopy (HREELS) system with the capability of two-dimensional (2D) energy and momentum mapping [25]. The HREELS measurements were performed along two high symmetry directions $\bar{\Gamma}-\bar{M}$ and $\bar{\Gamma}-\bar{K}$, as illustrated in the BZ shown in Fig. 1(a). Figures 1(c) and 1(d) show the HREELS 2D mapping of Bi_2Se_3 (0001) along two high symmetry directions where several energy loss peaks are labeled by α, OP, γ, and ζ. Figure 1(e) displays the energy distribution curves (EDCs) at $\bar{\Gamma}$, $\bar{K}$, and $\bar{M}$, respectively. The OP mode around 20 meV is almost dispersionless and assigned to an optical phonon of Bi_2Se_3, which corresponds to the A_{1g}^2 mode at Γ point in the Raman measurements [26] and is consistent with previous HREELS results [18]. The γ and ζ modes, around 55 and 72 meV without significant dispersions, are the conventional surface and bulk plasmon modes, respectively, originating from bulk conducting electrons [21]. These two modes, which have been observed but assigned to a single mode in Ref. [18], show strong damping and disappear at large q.

Distinct from the γ and ζ modes, the energy of α mode is strongly q dependent. As shown in Figs. 1(f) and 1(g) for both the energy-gain and loss sides, this α mode starts with zero energy at $\bar{\Gamma}$, disperses almost linearly along both the $\bar{\Gamma}-\bar{K}$ and $\bar{\Gamma}-\bar{M}$ directions. Even entering into the second BZ, this mode maintains the same linear dispersion without reflecting the lattice periodicity. This clearly indicates that the observed α mode is not an acoustic phonon, since the dispersion of an acoustic phonon must have the symmetry of the lattice. The observed dispersion of the α mode is the signature of plasmons.

To clarify the origin of the α mode, we performed HREELS measurements on Mn-doped Bi_2Se_3 (with 10% Mn doping). It is well known that Mn substitutes for Bi upon doping in the crystal structure [27–29]. Mn doping changes the properties of both electronic bands and collective excitations of the system. Especially, such magnetic doping breaks the time reversal symmetry so that the Dirac surface band opens a gap. Heavy doping such as around 10% used here completely demolishes the Dirac surface band, as shown from the ARPES data in the inset of Fig. 2(a), which is consistent with previously reported results [30]. Changes of the plasmons and phonons can also be seen in our results. Figure 2(a) shows the 2D HREELS energy-momentum mapping along the $\bar{\Gamma}-\bar{M}$ direction, while Fig. 2(b) displays the EDCs at the $\bar{\Gamma}$ point and $\bar{M}$ point. Compared with the HREELS results of Bi_2Se_3 [Fig. 1], the conventional surface and bulk plasmon modes γ and ζ exhibit the same dispersion behaviors, but their energies increase from 55 to 94 meV and

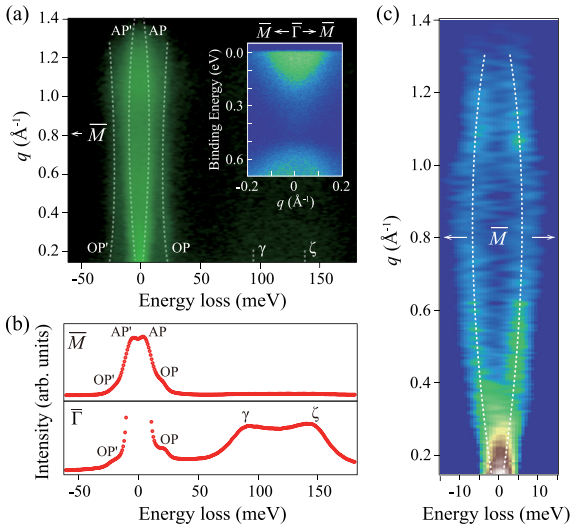

FIG. 2. Experimental results of Mn-doped Bi_2Se_3 (0001). (a) 2D energy-momentum mapping of HREELS measurements along the $\bar{\Gamma} - \bar{M}$ direction with the incident energy of 110 eV at room temperature. Four collective modes with energy loss features are labeled by AP, OP, γ, and ζ mode, respectively. The gray dashed lines are provided to guide to eye. The corresponding negative energy loss features are antistocks peaks of AP, OP modes, respectively, which are labeled by AP′, OP′. The inset is the band structure along the $\bar{M} - \bar{\Gamma} - \bar{M}$ direction measured by ARPES at 35 K, which shows that the V-shaped surface Dirac state disappears because of magnetic doping. (b) EDCs at $\bar{\Gamma}$ and $\bar{M}$ with corresponding energy loss peaks labeled. (c) The second derivative image of (a).

from 72 to 139 meV, respectively, owing to the increased bulk carrier density. This is evidenced by ARPES—the Fermi level is 0.15 eV above the conduction band minimum for Bi_2Se_3 [Fig. 1(b)], and 0.26 eV for Mn-doped Bi_2Se_3 [the inset of Fig. 2(a)]. While changes of the optical phonon (OP mode) caused by the Mn doping are mild, only showing slight linewidth broadening (~0.7 meV) and energy shift (~1 meV).

However, the most intriguing change are the characteristics of the low-energy feature on the Mn-doped Bi_2Se_3 (denoted as AP for acoustic phonon). It is fundamentally different from the originally observed α plasmon mode for Bi_2Se_3, although they are similar in energy and dispersion in the low q range. As clearly shown in Fig. 2(c), the energy of AP is symmetric with respect to the BZ, which is a signature of phonons. To summarize the difference, the dispersions of the α mode on Bi_2Se_3 and the AP mode on Mn-doped Bi_2Se_3 are plotted in Fig. 3(a). On the surface of Bi_2Se_3, where the topological surface states are present, the α plasmon mode appears, while the AP mode is suppressed. In contrast, on the surface of Mn-doped Bi_2Se_3 without the topological surface states, the α mode disappears and only the AP mode is present. Therefore, the α mode must originate from the topological surface states of Bi_2Se_3. In addition, from the measured dispersion curve of the AP mode [the pink curve in Fig. 3(a)], we extracted the sound velocity $v_s = 1610 \pm 90$ m/s by a linear fit of the data points for small q. Notice that for acoustic phonons it is only possible to obtain the transverse acoustic (TA) mode in HREELS measurements due to the restriction of the selection rules. Thus the AP mode is a TA mode with a transverse sound velocity of $\sim 1610 \pm 90$ m/s, which is very close to the reported value (1700 m/s) of Bi_2Se_3 [31,32].

The most striking behavior of the α mode is its slow attenuation in a large momentum range, which is in sharp contrast to the topologically trivial plasmon modes (i.e., γ and ζ modes). As shown in Figs. 3(c) and 3(d), the ζ mode's intensity drops drastically by more than 2 orders of magnitude when dispersing into the corresponding EHPC at 0.016 $Å^{-1}$ and diminishes beyond 0.08 $Å^{-1}$, and its linewidth increases correspondingly. Other plasmon modes generated by topologically trivial surface states, e.g., the 2D plasmon on the surface of Si(111)-$(\sqrt{3} \times \sqrt{3})$-Ag [22] or the acoustic plasmon on the surface of Be (0001) [34] show similar damping behavior. This is also true for the plasmon mode originated from Dirac electrons without topological protection, as is the case in graphene [7,35]. However, the α mode exhibits a small decrease in intensity when dispersing across the EHPC (0.00005 $Å^{-1} < q <$ 0.208 $Å^{-1}$) and remains observable far beyond. Furthermore, its linewidth is almost momentum independent [Fig. 3(d)]. In contrast to the AP mode, which clearly shows multiple-scattering matrix effects [21], the slow attenuation characteristics of the α mode are intrinsic, independent of the incident electron energy. Moreover, the intensity of the AP mode at room temperature (300 K) is obviously higher than that at low temperature (35 K), while the intensity of the α mode is almost temperature independent, strengthening the conclusion that the α mode observed in Bi_2Se_3 is not a simple phonon [21]. To understand why the α mode has an unusually long lifetime without fatal damping within the EHPC region, we should note that the Landau-type damping channels into the spin-unrestricted bulk band could be suppressed due to the spin-momentum locking restriction. Beyond the EHPC, the topological protection against any nonmagnetic impurity scattering also keeps the α mode from significant damping.

Another prominent characteristic of the α mode is its linear dispersion behavior in a large momentum range up to 2 $Å^{-1}$, independent of the periodicity of the lattice. However, the dispersion slope of the α mode (i.e., the velocity of the mode) is well over an order of magnitude smaller than that calculated from the continuous medium excitation picture [15,33,36]. This is also in sharp contrast to the case of the 2D plasmon mode from the Dirac electrons in graphene [7], where the dispersion is larger than theoretical calculations.

A possible interpretation of such anomalously small energy dispersion of the α mode is a coupling with other collective excitations, which results in a severe self-energy renormalization. Since its energy is close to that of the

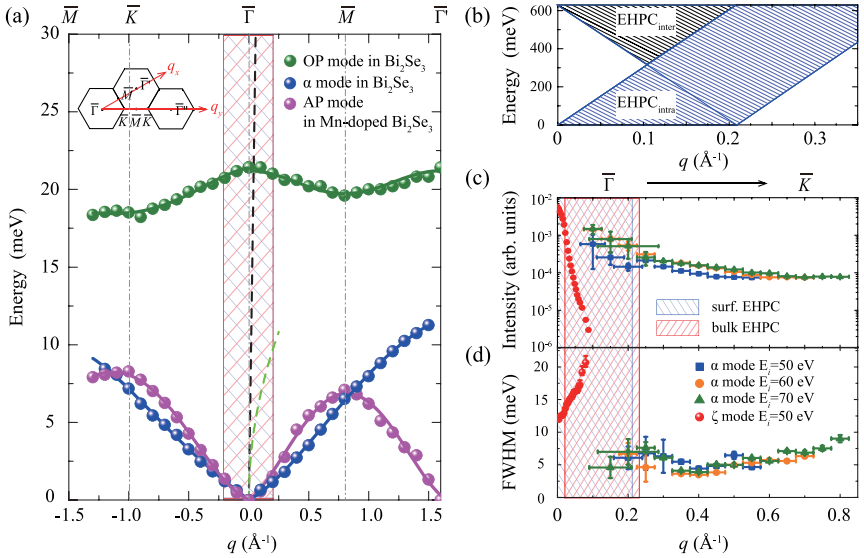

FIG. 3. Characteristics of the α plasmon mode. (a) The dispersions of the α mode, OP mode of Bi_2Se_3, and the AP mode of Mn-doped Bi_2Se_3. The dispersions of theoretically predicted Dirac plasmon and spin-plasmon are calculated by simply extrapolating the momentum range of the equations in Refs. [33] and [15], and plotted as black and green dashed lines, respectively. The shaded zones label the EHPC of massless Dirac electrons and normal bulk conducting electrons. (b) The enlarged EHPC of massless Dirac electrons in an extended energy range. (c) The normalized intensity and (d) FWHM of the α mode of Bi_2Se_3 with different incident energies. The shaded zones illustrate the EHPC of Dirac surface electrons and normal bulk conducting electrons, respectively. The normalized intensity and FWHM of the bulk plasmon (ζ mode) of Bi_2Se_3 are also plotted for comparison.

surface phonons, the α mode is likely to interact strongly with this excitation. This can be qualitatively understood by considering a plasmon dressed by a phonon mode due to strong electron-lattice interaction [37]. As a result, the plasmon frequency should be $\omega_q = [\omega_{pl}/\sqrt{\epsilon_i(\omega, q)}]$, where ω_{pl} is the bare or undressed frequency, and $\epsilon_i(\omega, q)$ the ionic effective dielectric function [38]. In a 2D electron liquid picture with short-range interactions [15,36], the bare plasmon was theoretically predicted to have acoustic dispersion (for $q < k_F$, the Fermi wave vector), $\omega_{pl} \approx v_F q$, where v_F is the Fermi velocity. But these theories are based on random phase approximation so that they can only obtain the dispersions for small q, and neglect possible electron-lattice interactions. In Bi_2Se_3, a considerable number of studies [39–44] have shown both theoretically and experimentally that the surface Dirac states interact strongly with surface phonons, although the specific values of the electron phonon coupling constant and the interaction mechanism are still under debate [45]. With strong electron-lattice interaction, $\epsilon_i(\omega, q) \propto (\Omega/\omega_i)^2 \gg 1$, where Ω represents the interaction strength and ω_i the phonon energy. Then the plasmon dispersion becomes $\omega_q \approx (\omega_i/\Omega) v_F q$, so it remains acoustic, but its slope (velocity) can be strongly reduced by electron-lattice interaction. Indeed, as shown in Figs. 1(f) and 1(g) as well as Fig. 3, the dispersion of the α mode is slightly anisotropic, e.g., the energy at $q = 1.2$ Å^{-1} is 9.6 meV along the $\bar{\Gamma} - \bar{M}$ direction as compared to 8.5 meV along the $\bar{\Gamma} - \bar{K}$ direction. This indicates the effects of lattice symmetry, which manifests the topological protection of the observed collective mode. However, whether or not the α mode couples with a spin density wave remains unclear. Our observations demonstrate both the surface Dirac states and their collective excitations are topologically protected on the 3D TI, though more quantitative studies are needed.

We thank M. El-Batanouny, Z. Fang, Z. Wang, H. Weng, Y. Ran, and C. Fang for helpful discussions. The work was supported by the National Key Research and Development Program of China (No. 2016YFA0302400 and No. 2016YFA0300600), the National Natural Science Foundation of China (No. 11304367, No. 11634016, and No. 11474334), and the Strategic Priority Research Program (B) of CAS (Grant No. XDB07010100). X. Z. was partially supported by the Youth Innovation Promotion Association of Chinese Academy of Sciences. J. Z. was supported by U.S. NSF under Grant No. DMR 1608865, and sabbatical program of the Institute of Physics, Chinese Academy of Sciences.

*To whom correspondence should be addressed.
xtzhu@iphy.ac.cn
†jdguo@iphy.ac.cn

[1] D. Pines and D. Bohm, Phys. Rev. **85**, 338 (1952).
[2] R. H. Ritchie, Phys. Rev. **106**, 874 (1957).
[3] L. Landau, Sov. Phys. JETP **3**, 920 (1957).
[4] D. Pines and P. Nozières, *The Theory of Quantum Liquids: Normal Fermi Liquids* (W.A. Benjamin, New York, 1966), Vol. 1.

[5] B. W. Ninham, C. J. Powell, and N. Swanson, Phys. Rev. **145**, 209 (1966).
[6] R. H. Ritchie, Surf. Sci. **34**, 1 (1973).
[7] Y. Liu, R. F. Willis, K. V. Emtsev, and T. Seyller, Phys. Rev. B **78**, 201403 (2008).
[8] H. Zhang, C.-X. Liu, X.-L. Qi, X. Dai, Z. Fang, and S.-C. Zhang, Nat. Phys. **5**, 438 (2009).
[9] Y. L. Chen *et al.*, Science **325**, 178 (2009).
[10] Y. Xia *et al.*, Nat. Phys. **5**, 398 (2009).
[11] D. Hsieh *et al.*, Science **323**, 919 (2009).
[12] P. Roushan, J. Seo, C. V. Parker, Y. S. Hor, D. Hsieh, D. Qian, A. Richardella, M. Z. Hasan, R. J. Cava, and A. Yazdani, Nature (London) **460**, 1106 (2009).
[13] T. Zhang *et al.*, Phys. Rev. Lett. **103**, 266803 (2009).
[14] Y. Okada and V. Madhavan, Nat. Nanotechnol. **8**, 541 (2013).
[15] S. Raghu, S. B. Chung, X. L. Qi, and S. C. Zhang, Phys. Rev. Lett. **104**, 116401 (2010).
[16] P. Di Pietro *et al.*, Nat. Nanotechnol. **8**, 556 (2013).
[17] A. Politano, V. M. Silkin, I. A. Nechaev, M. S. Vitiello, L. Viti, Z. S. Aliev, M. B. Babanly, G. Chiarello, P. M. Echenique, and E. V. Chulkov, Phys. Rev. Lett. **115**, 216802 (2015).
[18] A. Kogar *et al.*, Phys. Rev. Lett. **115**, 257402 (2015).
[19] Y. D. Glinka, S. Babakiray, T. A. Johnson, M. B. Holcomb, and D. Lederman, Nat. Commun. **7**, 13054 (2016).
[20] F. T. Huang, M. W. Chu, H. H. Kung, W. L. Lee, R. Sankar, S. C. Liou, K. K. Wu, Y. K. Kuo, and F. C. Chou, Phys. Rev. B **86**, 081104 (2012).
[21] See Supplemental Material at http://link.aps.org/supplemental/10.1103/PhysRevLett.119.136805 for details, which includes Refs. [18,20,22–24].
[22] T. Nagao, T. Hildebrandt, M. Henzler, and S. Hasegawa, Phys. Rev. Lett. **86**, 5747 (2001).
[23] W. Richter and C. R. Becker, Phys. Status Solidi B **84**, 619 (1977).
[24] M. Stordeur, K. K. Ketavong, A. Priemuth, H. Sobotta, and V. Riede, Phys. Status Solidi B **169**, 505 (1992).
[25] X. Zhu, Y. Cao, S. Zhang, X. Jia, Q. Guo, F. Yang, L. Zhu, J. Zhang, E. W. Plummer, and J. Guo, Rev. Sci. Instrum. **86**, 083902 (2015).
[26] J. Zhang, Z. P. Peng, A. Soni, Y. Y. Zhao, Y. Xiong, B. Peng, J. B. Wang, M. S. Dresselhaus, and Q. H. Xiong, Nano Lett. **11**, 2407 (2011).
[27] Y. S. Hor *et al.*, Phys. Rev. B **81**, 195203 (2010).
[28] L. J. Collins-McIntyre *et al.*, AIP Adv. **4**, 127136 (2014).
[29] S. F. Qi, H. L. Yang, J. Chen, X. Y. Zhang, Y. P. Yang, and X. H. Xu, Sci. Rep. **6**, 29161 (2016).
[30] S.-Y. Xu *et al.*, Nat. Phys. **8**, 616 (2012).
[31] S. Giraud, A. Kundu, and R. Egger, Phys. Rev. B **85**, 035441 (2012).
[32] Y. D. Glinka, S. Babakiray, T. A. Johnson, M. B. Holcomb, and D. Lederman, J. Appl. Phys. **117**, 165703 (2015).
[33] S. Das Sarma and E. H. Hwang, Phys. Rev. Lett. **102**, 206412 (2009).
[34] B. Diaconescu *et al.*, Nature (London) **448**, 57 (2007).
[35] C. Tegenkamp, H. Pfnur, T. Langer, J. Baringhaus, and H. W. Schumacher, J. Phys. Condens. Matter **23**, 012001 (2011).
[36] D. K. Efimkin, Y. E. Lozovik, and A. A. Sokolik, Nanoscale Res. Lett. **7**, 163 (2012).
[37] R. D. Mattuck, *A Guide to Feynman Diagrams in the Many-Body Problem* (Courier Corporation, New York, 2012).
[38] G. D. Mahan, *Many-Particle Physics* (Springer Science & Business Media, New York, 2013).
[39] S. Giraud and R. Egger, Phys. Rev. B **83**, 245322 (2011).
[40] R. C. Hatch, M. Bianchi, D. D. Guan, S. N. Bao, J. L. Mi, B. B. Iversen, L. Nilsson, L. Hornekaer, and P. Hofmann, Phys. Rev. B **83**, 241303 (2011).
[41] X. T. Zhu, L. Santos, C. Howard, R. Sankar, F. C. Chou, C. Chamon, and M. El-Batanouny, Phys. Rev. Lett. **108**, 185501 (2012).
[42] T. Kondo *et al.*, Phys. Rev. Lett. **110**, 217601 (2013).
[43] M. V. Costache, I. Neumann, J. F. Sierra, V. Marinova, M. M. Gospodinov, S. Roche, and S. O. Valenzuela, Phys. Rev. Lett. **112**, 086601 (2014).
[44] J. A. Sobota, S. L. Yang, D. Leuenberger, A. F. Kemper, J. G. Analytis, I. R. Fisher, P. S. Kirchmann, T. P. Devereaux, and Z. X. Shen, Phys. Rev. Lett. **113**, 157401 (2014).
[45] R. Heid, I. Y. Sklyadneva, and E. V. Chulkov, Sci. Rep. **7**, 1095 (2017).